Title

Comparative studies of T = 3 and T = 4 icosahedral RNA insect viruses

Authors

Johnson, JE
Munshi, S
Liljas, L
et al.

Publication Date

1994

DOI

10.1007/978-3-7091-9326-6_48

Peer reviewed

Arch Virol (1994) [Suppl] 9: 497–512

Archives of Virology

Comparative studies of $T = 3$ and $T = 4$ icosahedral RNA insect viruses

J. E. Johnson, S. Munshi, L. Liljas*, D. Agrawal, N. H. Olson, V. Reddy, A. Fisher, B. McKinney, T. Schmidt,** and **T. S. Baker**

Department of Biological Sciences, Purdue University, West Lafayette, Indiana, U.S.A.

Summary. Crystallographic and molecular biological studies of $T = 3$ nodaviruses (180 identical subunits in the particle) and $T = 4$ tetraviruses (240 identical subunits in the particle) have revealed similarity in both the architecture of the particles and the strategy for maturation. The comparative studies provide a novel opportunity to examine an apparent evolution of particle size, from smaller ($T = 3$) to larger ($T = 4$), with both particles based on similar subunits. The BBV and FHV nodavirus structures are refined at 2.8 Å and 3 Å respectively, while the NωV structure is at 6 Å resolution. Nevertheless, the detailed comparisons of the noda and tetravirus X-ray electron density maps show that the same type of switching in subunit twofold contacts is used in the $T = 3$ and $T = 4$ capsids, although differences must exist between quasi and icosahedral threefold contacts in the $T = 4$ particle that have not yet been detected. The analyses of primary and tertiary structures of noda and tetraviruses show that NωV subunits undergo a post assembly cleavage like that observed in nodaviruses and that the cleaved 76 C-terminal residues remain associated with the particle.

Introduction

There are a variety of unifying themes in the structure and function of positive strand RNA viruses and these have been used to construct

Present addresses: * University of Uppsala, Biomedical Center, Department of Molecular Biology, Uppsala, Sweden; ** Institute for Enzyme Research, University of Wisconsin, Madison, Wisconsin, U.S.A.

detailed evolutionary relationships among these viruses [1, 2]. Most positive strand RNA viruses have icosahedral capsids with $T = 3$ quasi symmetry (primarily plant viruses) or a picornavirus type capsid (primarily animal viruses) [2]. These capsid types are themselves related, with an apparent triplication of the capsid protein gene observed in the $T = 3$ viruses forming the picornavirus capsids [3]. The identification of a particular capsid type with viruses infecting members of a particular kingdom is not universal, however, since there are plant viruses with capsids that are clearly related to the picornaviruses [4] and there are animal viruses with $T = 3$ symmetry [5, 6]. Because there are such limited examples of capsid types the only comparisons to date have been between $T = 3$ and picornavirus capsids [2, 3, 4]. We have been investigating two groups of insect viruses, nodaviruses [7] (displaying $T = 3$ quasisymmetry) and tetraviruses [8] (displaying $T = 4$ quasisymmetry). In this paper we report similarities in structure and function that are apparent from our biochemical and biophysical studies.

The $T = 3$ nodaviruses are among the simplest animal viruses known. Their genomes consist of roughly 4500 bases that are split between two single-stranded, messenger-sense RNA molecules encapsidated in one virion [9]. The genome encodes only three proteins [10]; a replicase (protein A), the coat protein precursor (protein α) and a protein of unknown function (protein B). Nodaviruses are small non-enveloped viruses that infect insects [7], mice [11], and fish [12]. They can be produced in large quantity and readily crystallized. They undergo a well characterized series of assembly and maturation steps [13]. An infectious clone is available for Flock House nodavirus (FHV) [14], and particles spontaneously assemble and package their own messenger RNA when the FHV capsid protein gene is expressed in a baculovirus system [15]. The structure of the black beetle nodavirus (BBV) has been determined [5] and was found to be similar to all $T = 3$ RNA plant virus structures analyzed, although the β-barrel subunits contained elaborate surface loops and an interior helical domain not observed in the plant viruses. Biochemical studies of FHV showed that 80% of the coat protein subunits α (407 amino acids) underwent a post assembly, autocatalytic cleavage to form protein β (363 amino acids) and protein γ (44 amino acids) in the mature virion and that this cleavage was required for infectivity [16]. This maturation is similar to that observed in picornaviruses [17] and suggests that the nodaviruses, although displaying a different capsid architecture, may share a common biological strategy for particle maturation and possibly uncoating.

The *Tetraviridae* family of viruses, formerly referred to as the *Nudaurelia* β virus family, consists of seven members that from icosahedral particles with $T = 4$ symmetry [8]. All members of this virus group

identified to date propagate exclusively in insect hosts. The prototype, *Nudaurelia capensis* β virus (NβV), was originally isolated from the pine emperor moth, *Nudaurelia cytharea capensis* Stoll [18] and it has been the subject of recent studies [19]. This group of viruses form shells that are 350–400 Å in diameter, encapsidating a single-stranded RNA having a molecular mass of $1.8–1.9 \times 10^6$ daltons. The particles have sedimentation coefficients between 200S and 210S. Examination of the capsids by SDS-PAGE revealed in all cases a single capsid polypeptide estimated to be 65–68 kD. Compilations of these characteristics for individual members have recently been published [20, 21].

The striking differences between noda and tetraviruses are the size of the capsid subunit and the size of the particle (Table 1). Earlier work on these viruses did not suggest a relationship between them, however, structural studies at the primary and tertiary level of *Nudaurelia capensis* ω virus (NωV), another tetravirus, now suggest that noda and tetraviruses are related [22]. The geometric concepts for generating quasi equivalent shells have been developed on the basis of theoretical and experimental data [23, 24]. The nodaviruses display $T = 3$ symmetry (180 subunits in the capsid) and the tetraviruses $T = 4$ symmetry (240 subunits in the capsid). The first two high resolution virus structures determined were for the $T = 3$ plant viruses, tomato bushy stunt virus [25] and southern bean mosaic virus [26]. Remarkably, they were found to have subunit tertiary and particle quaternary structures that were virtually superimposable in the contiguous shell, although the subunits displayed only limited sequence homology. The $T = 3$ plant and animal viruses have a shape that is strikingly similar to the rhombic triacontahedron [27] and this geometric solid is shown and discussed in Figs. 1a and b. Although structurally similar to the plant viruses in many respects, recent studies have shown that nodaviruses incorporated regions of duplex RNA in the capsid and that the RNA functioned as part of the molecular switch that regulates the formation of the $T = 3$ shell [28].

Comparison of subunit primary structures of noda and tetravirus

The segmented genome of NωV consists of RNA1 (5 kb) and RNA2 (2.5 kb). The sequence of RNA2 was recently reported and the encoded amino acid sequence was compared with nodavirus capsid proteins [22]. Two similarities were observed. First, the NωV coat protein (646 residues) probably undergoes a post translational cleavage. This was apparent when the virus particle was subjected to direct chemical protein sequencing. The 21 "Nterminal" amino acids obtained in this experiment aligned with residues 571 to 591 encoded by the RNA2 gene. The likely explanation for this result is that a posttranslational cleavage occurs

Table 1. A comparison of features between *Nodaviridae*, NωV, and NβV

Virus	Icosahedral symmetry	Number of subunits	Particle size (Å)	Buoyant density (g/cc)	Polypeptide composition	Genomic composition	Encoded products
Nodaviridae	$T = 3$	180	312 (9.4×10^6 mD)	1.33	β (38 kD) γ (5 kD)	RNA1 (3.1 kb) RNA2 (1.4 kb)	protein A, B α (β,γ)
NωV	$T = 4$	240	410	1.285	β (62 kD) γ (8 kD)	RNA1 (5 kb) RNA2 (2.5 kb)	n.d. α (β,γ)
NβV	$T = 4$	240	397 (16.3×10^6 mD)	1.295	β (61 kD) γ (8 kD)	RNA1 (5.4 kb)	n.d.

n.d. Not determined

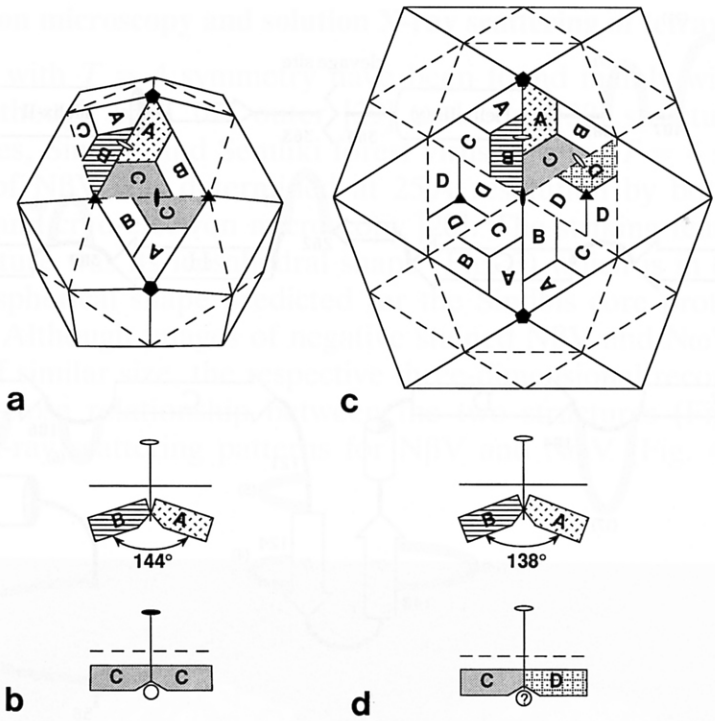

Fig. 1. Diagrammatic representations of the subunit associations accounting for contiguous shells in $T = 3$ (**a, b**) and $T = 4$ icosahedrons (**c, d**). Labeled trapezoids represent the individual capsid subunits. The packing relations, as viewed along an equatorial line within the structure, between *C* subunits related by the icosahedral twofold (solid ellipse) and between *A* and *B* subunits related by the quasi twofold (open ellipse) are shown for the $T = 3$ structure in **b**. Likewise, the *C* and *D*, and the *A* and *B* subunits of the $T = 4$ structure, related by different quasi twofold axes, are shown in **d**. A peptide and RNA duplex (open circle, **b**) maintains the planar *C-C* contact as observed in the BBV structure [4]. A similar peptide (**d**) may keep the *C-D* contact in the $T = 4$ structure planar. Open and closed ellipses, closed triangles, and closed pentagons represent quasi and icosahedral twofold, and icosahedral threefold and fivefold axes, respectively

between residues 570 and 571, making residue 571 an unblocked N-terminus of a polypeptide consisting of residues 571–646 (This would correspond to the γ peptide described for nodaviruses). The true N-terminus of the NωV coat protein translation product is probably blocked like many other viral capsid proteins. Exactly this situation was found with the Flock House nodavirus [13]. When NωV was analyzed on a SDS gel, there was clear evidence for a small polypeptide of molecular weight ~8 kD as well as the larger polypeptide at ~61 kD. Earlier studies had not reported the small protein probably because it ran off the end of the gel under typical electrophoresis conditions. The gene for the NωV capsid protein has been cloned and expressed in *E. coli* and the resultant

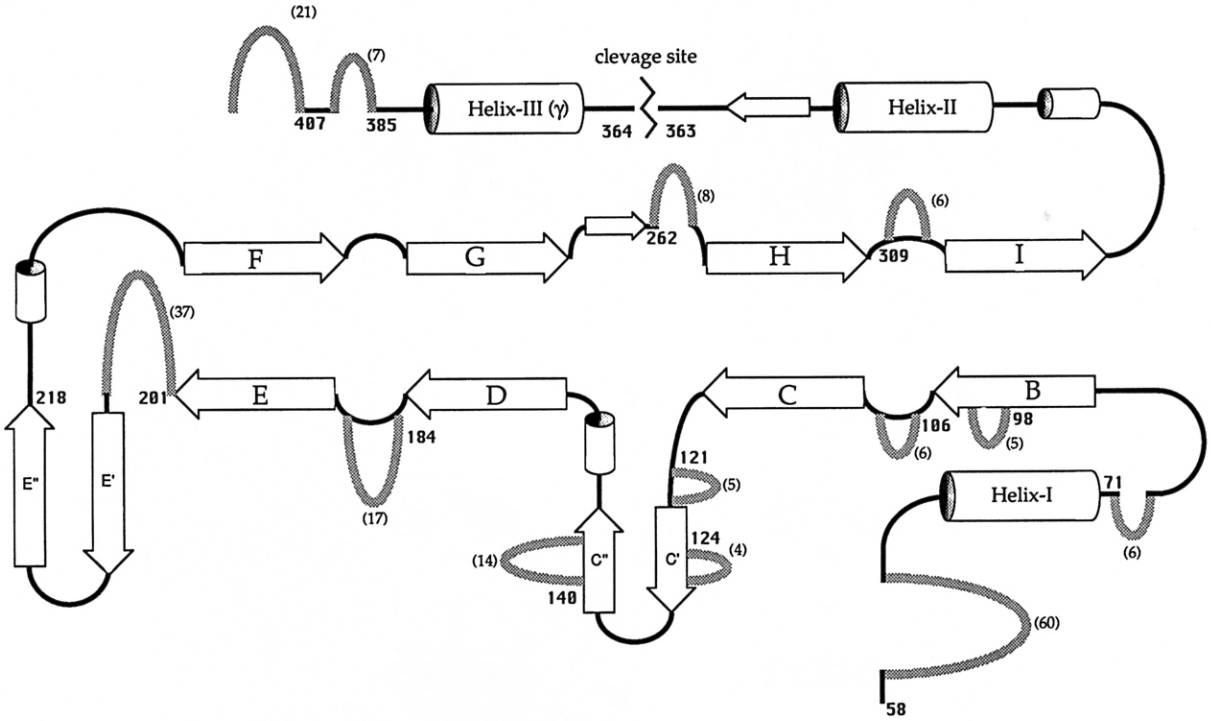

Fig. 2. A schematic representation of secondary structure elements observed in BBV[5] and FHV[28]. Stipled lines show the positions (in the BBV sequence) and the number of residues inserted in the capsid protein of NωV on the basis of the primary structure alignment. Note the alignment places all but one of the insertions between secondary structure elements suggesting that the β-structure is conserved in noda and tetraviruses

gene product is a 71 kD protein that reacts with antibodies to NωV particles in a western blot. The NωV sequence was aligned with the four nodavirus sequences by the program PILEUP. Although the number of amino acids in the nodavirus capsid protein is roughly 400 and the number in the NωV capsid protein is 646, a significant level of similarity was found. Two aspects of the alignment were notable. First, virtually all of the additional amino acids in NωV were accounted for by inserts between strands of the β-barrel in the known structures of the nodaviruses. This suggests that the residues of the β-barrel strands are relatively conserved and that the additional mass of the NωV protein is composed of insertions between these strands. Significant inserts also are located at the beginning and at the end of the β-barrel. The relation between the BBV secondary structures and the NωV inserts is shown in Fig. 2. Another remarkable feature of the alignment is the coincidence of the cleavage sites, located between residues N363 and A364 in BBV and FHV and between residues N570 and F571 in NωV.

Electron microscopy and solution X-ray scattering of tetraviruses

Structures with $T = 4$ symmetry have been found mainly within insect viruses, although both the outer [29] and core [30] structures of the alphaviruses, Sindbis and Semliki forest virus, display $T = 4$ shells. The structure of NβV was determined at 25 Å resolution by both negative stain [31] and cryo-electron microscopy [20]. The striking feature of the NβV structure was its icosahedral shape (Fig. 3) which is in contrast to the more spherical shape predicted for the Sindbis core protein $T = 4$ shell [30]. Although images of negative stained NβV and NωV revealed particles of similar size, the respective three-dimensional reconstructions showed a close relationship between the two structures (Fig. 3). The solution X-ray scattering patterns for NβV and NωV (Fig. 4) are also

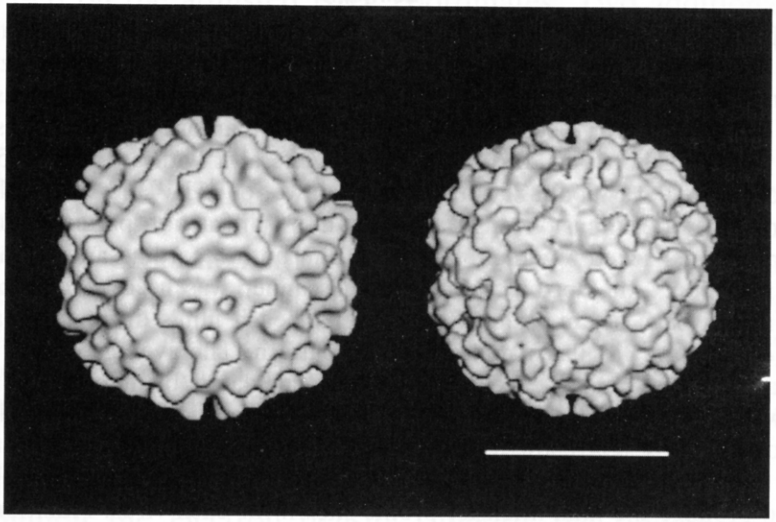

Fig. 3. Shaded-surface representations of three-dimensional reconstructions of NβV (left) and NωV (right) computed from images of frozen-hydrated virions. The bar on the right is 250 Å. Specimens were prepared for cryo-electron microscopy by applying small drops of each sample to perforated carbon films on 400 mesh copper grids. The grids were briefly blotted with filter paper and then rapidly plunged into liquified ethane. They were then transferred to liquid nitrogen before being inserted into a cold, Gatan cryotransfer holder and then into a Philips EM420 transmission electron microscope. The images were recorded at ~1.5 μm underfocus, at 49 000X magnification, and with an electron dose of ~20e^{-}/Å^2. Selected micrographs were digitized, individual particle images from each were boxed, and the background density of each image was subtracted. The initial centers of density of each image were determined by cross correlation methods [36] and the orientation of each particle, with respect to the view axis, was determined with established icosahedral processing procedures [37–39]. Refined data sets of twenty-five images of NβV and 57 of NωV were used to calculate three-dimensional reconstructions of each virus with an effective resolution of 31 Å and 28 Å, respectively

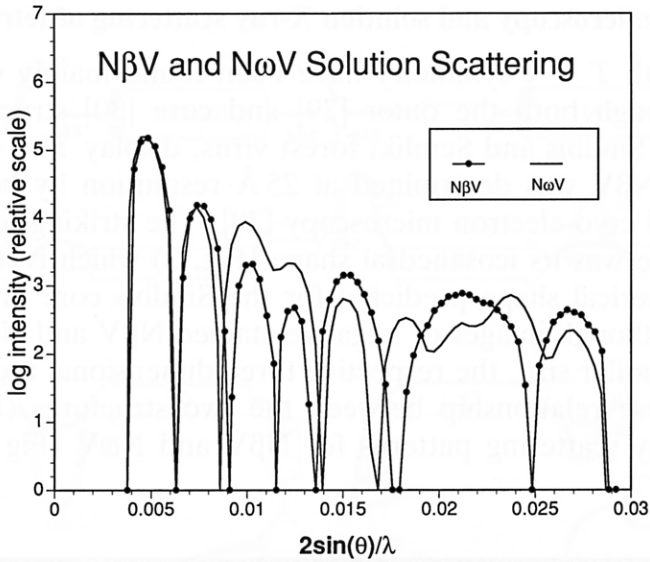

Fig. 4. NβV and NωV solution scattering patterns. Each virus was pelleted, resuspended in buffer at approximately 150 mg/ml, and placed in a 1 mm quartz capillary. Diffraction data were then collected, at 267.5 mm sample-to-film distance, using CuKa radiation, a double-mirror focusing camera [40, 41] with an order-to-order resolution of ~1 500 Å, and an Elliott GX-20 rotating anode generator with a 0.15 × 2.5 mm focal spot. Exposure time was about 85 h at an X-ray power of 35 kV and 30 mA. In order to fully record the wide intensity range of each virus's diffraction pattern, three Kodak DEF-5 films were stacked together, with each film both recording and attenuating the scattered radiation. An Optronics C4100 film scanner was used to digitize the film optical densities on a 50 μm raster. The center of each film's diffraction pattern was determined using the circular symmetry of the pattern. The average optical density at each radial distance from the center was then calculated by integrating all optical densities within 50 μm thick circular shells. Each film's final radial intensity distribution was then obtained by subtracting a smooth background curve fitted through the nodes. The three radial intensity distributions (from the three stacked films) were then scaled together to produce the final intensity profile shown for each virus. Additional experimental details can be found in [42]

different, but display an underlying similarity consistent with the electron microscopy reconstructions.

Figures 1c and d represent the tetravirus $T = 4$ structure diagrammatically and show the similarity with the rhombic triacontahedron of the $T = 3$ structure. On the basis of this comparison a detailed model of the NωV $T = 4$ shell was constructed with the subunit tertiary structure observed in the $T = 3$ shell of BBV [5]. The icosahedral asymmetric unit of the $T = 4$ shell (A, B, C, D) (Fig. 1c) was defined as the A, B, C and C2 subunits in the $T = 3$ shell (Fig. 1a). The coordinates of atoms in these four subunits in BBV were adjusted radially until a non-overlapping contiguous shell was formed with atoms in neighboring asymmetric units

generated by the icosahedral symmetry operations. Table 2 lists the coordinates and radial distances of well-defined features observed in the subunits of BBV as they were positioned in the $T = 4$ NωV modeled structure. These are compared with features in the electron density map of NωV below.

Electron density of NωV at 8 Å resolution

Crystals of NβV and NωV have been produced and they diffract X-rays to 2.7 Å resolution [32, 33]. Both viruses crystallize in an unusual but similar unit cell. Cell dimensions and crystallization conditions are given in Table 3. The proposed similarity of the noda and tetraviruses is supported by the 8 Å resolution NωV electron density map recently computed. There is clear evidence for a β-barrel core in the electron density for the contiguous shell of NωV and it agrees well with the $T = 4$ model based on the adjusted BBV coordinates. Two additional characteristics found in nodavirus structures that were obvious in the 8 Å electron density map were the helical interior domain that probably contains the C terminal portion of the cleaved capsid protein γ (residues 571 to 646) and a peculiar "doughnut" shaped density feature surrounding the fivefold symmetry axes. Both of these features were clear in the NωV map (Figs. 5a and b) and they served as markers to compare the model of NωV generated with the BBV subunits with the actual NωV structure. The γ peptides of the BBV subunits are placed in helical density in the NωV map (Fig. 5a). In addition the leucine residues on the βD-βE loop of BBV are directly in contact with the "doughnut" shaped density appearing in that structure about the fivefold axes, and the BBV subunits modeled in the NωV map occupy exactly the same position relative to the "doughnut" shaped density in NωV (Fig. 5b). Thus, at 8 Å resolution the electron density supports the similarities between nodaviruses and tetraviruses based on geometric arguments and the sequence alignments.

Discussion

The noda and tetravirus systems offer a unique opportunity to study the factors affecting capsid architecture. Evidence presented here suggests that the subunit building blocks of noda and tetraviruses are similar, particularly with regard to the β-barrel that forms the contiguous protein shell. Other features of the $T = 3$ and $T = 4$ shells, in addition to the β-barrel, are also comparable. These include the helical domain that lies inside the barrel, which is the location of the autocatalytic maturation cleavage in FHV and BBV, and the "doughnut" shaped density that exists on the fivefold symmetry axes in nodavirus structures and NωV.

Table 2. NωV ($T = 4$) model based on BBV

	Residue # (Cα)	X	Y	Z	D (Å)
Farthest distance along Q3	B207	59.	−1.	183.	192.
Farthest distance along I5	A306	103.	−3.	163.	193.
Farthest distance along I3	C207	−2.	1.	183.	183.
Farthest distance along I2	A305	18.	−42.	159.	165.
γ Peptide of A subunit	A379	76.	−3.	119.	142.
	A364	92.	2.	133.	161.
Doughnut along I5	A182	108.	−0.	154.	188.
	A181	106.	1.	150.	184.
Ca^{2+} on Q3 axis	A249	62.	1.	141.	154.
	A251	61.	5.	145.	157.
Residue (measured at)	**strand**	**X**	**Y**	**Z**	**D (Å)**
CHEF-sheet of β-barrel of a subunit					
190	E	85.	−6.	150.	173.
299	H	85.	−3.	154.	176.
113	C	84.	1.	157.	178.
277	F	48.	19.	165.	173.
BIDG-sheet of β-barrel of a subunit					
241	G	84.	0.	145.	167.
174	D	87.	6.	147.	172.
314	I	86.	9.	150.	173.
100	B	87.	13.	152.	176.
Loops facing fivefold axis measured at	**loop**	**X**	**Y**	**Z**	**D (Å)**
108	βB-βC	96.	−5.	165.	191.
306	βH-βI	103.	−3.	163.	193.
183	βD-βE	105.	1.	156.	188.
236	βF-βG	98.	−0.	149.	178.
135	βC-βC′	80.	−9.	168.	186.

Heavy atom positions (site)	X	Y	Z	D (Å)
A	99.	2.	164.	192.
B	38.	−38.	166.	174.
C	34.	36.	164.	171.
D	24.	−36.	166.	172.

Sites A, B and C are related by quasi threefold symmetry and sites C and D by quasi twofold symmetry

Table 3. Tetravirus crystals

Crystal form (virus)	Space group	Lattice constants	Z
Form III NβV[a]	P1	408.7 Å, 403.14 Å, 409.67 Å, 59.35°, 58.97°, 63.21°	1
NωV[b]	P1	413.55 Å, 410.22 Å, 419.67 Å, 59.13°, 58.9°, 64.04°	1

[a] Growth conditions: Virus (8–14 mg/ml) in 0.07 M acetate buffer pH 5.0 (V) precipitated by vapor diffusion with 0.1 M $Ca(NO_3)_2$, 2.25% PEG 8000 and 0.5% β-octyl glucoside in acetate buffer pH 5.0 (P). Ratio of virus to precipitant solution in drop (V:P = 1:1), vapor equilibrated against P

[b] Growth conditions: Virus (8–10 mg/ml) in 0.07 M acetate buffer pH 5.0 (V) precipitated by vapor diffusion with 2% PEG 8000, 0.25 M $CaCl_2$ and 0.001 M NaN_3 in 0.075 M morpholino propanesulfonic acid (MOPS) buffer pH 7.0 (P). Ratio of virus to precipitant solution in drop (V:P = 1:4), vapor equilibrated against P

Biochemical and structural studies of nodaviruses have suggested a mechanism for the autocatalytic cleavage that involves an acid-catalyzed main-chain hydrolysis event. The cleavage is also required for infectivity in nodaviruses and results in a substantial increase in particle stability. By analogy a similar maturation mechanism can be predicted for NωV. Unfortunately, it has not been possible to propagate NωV in any cell line, so the study of its biochemical and biological properties has not been possible. Schneemann et al. [15] have shown that when the capsid protein gene of FHV is expressed in a baculovirus system the subunits spontaneously assemble and package the messenger RNA for the capsid protein gene. The expression of the wild type sequence of the FHV capsid protein gene results in normal subunit processing and maturation. Mutation of the asparagine(N) at residue 363 to threonine(T), alanine, or aspartic acid result in cleavage inhibition. The N363T mutant expressed in baculovirus is stable as the provirion and this particle type has been crystallized [34]. Currently we are attempting to express the capsid gene of NωV in a baculovirus system and we anticipate that these subunits will assemble to form a $T = 4$ capsid, thus permitting a thorough study of factors affecting the assembly and architecture of a $T = 4$ shell. Such a study is currently being done for the $T = 3$ shell of FHV [35].

The $T = 4$ architecture is intriguing when viewed as the simplified model in Fig. 1. Finch et al. [31] recognized that the icosahedral asymmetric unit of tetraviruses (containing four subunits) does not form a logical assembly unit, and they suggested that the particle may form from preassembled trimers. This assembly hypothesis is consistent with the $T = 4$ organization described here. The detailed model predicts that, prior to assembly, there is probably no difference between trimers

related by icosahedral symmetry (DDD) and trimers related by quasi threefold symmetry (ABC) (Fig. 1c) and it is only after the shell starts to assemble that the two classes of trimers begin to differ slightly. The nature of the two classes of quasi twofold axes (bent and flat) in the $T = 4$ particle are nearly identical to the quasi (bent) and icosahedral (flat) twofold axes in the $T = 3$ nodaviruses (Fig. 1). The nodaviruses architecture results from ordered RNA and a 10 amino acid polypeptide that are visible only at the "flat" contact between trimers at the icosahedral twofold axes. At the "bent" quasi twofold axes the RNA and protein polypeptide do not obey icosahedral symmetry and are invisible. Portions of the capsid protein that interact with the RNA and polypeptide at the

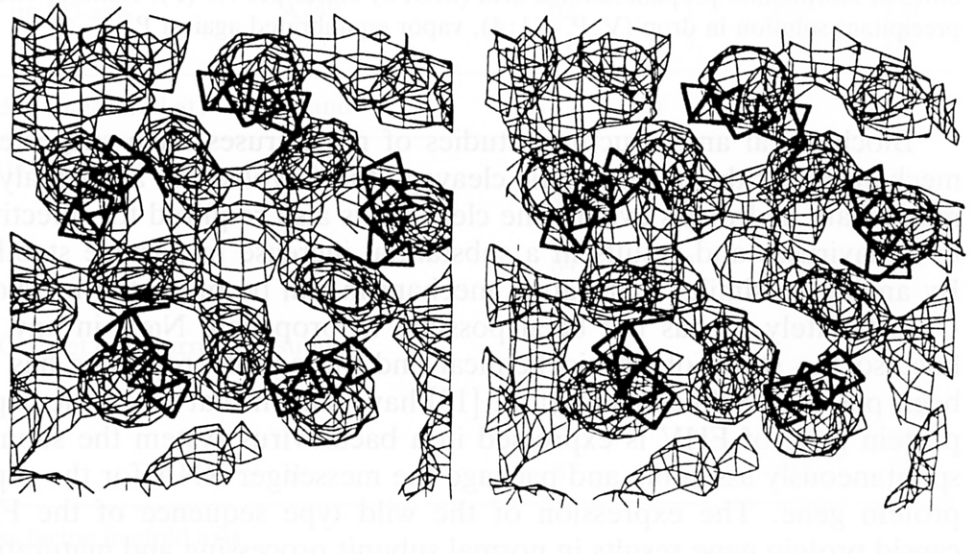

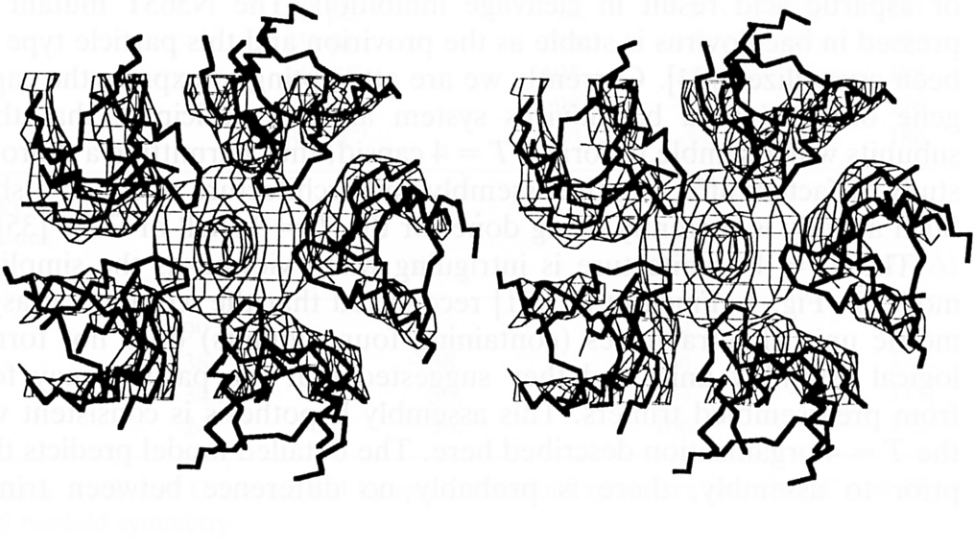

flat contact interact with each other at the bent contact. A similar mechanism can be invoked for formation of bent and flat contacts in $T = 4$ structures (Fig. 1b), but at present we have no suggestion for differentiating the two trimers. The difference between $T = 3$ and $T = 4$ structures is apparent at the quasi sixfold axes, which exist in both. In $T = 3$ shells the quasi sixfold axis is coincidental with an icosahedral threefold axis and the actual structure is best described as a trimer of BC dimers. The quasi sixfold axis in the $T = 4$ shell is coincident with an icosahedral twofold axis and thus is probably best described as a dimer of BCD trimers. The 2.8 Å structure of NωV should clearly show what portions of the coat protein or RNA regulate this aspect of the $T = 4$ particle.

Acknowledgements

We thank D. Hendry for supplying samples of *Nudaurelia capensis* ω virus, and S. Fateley for help in preparing the manuscript. This work was supported by a NIH grant (GM34220) to JEJ.

Fig. 5. Features in the electron density map of NωV. The electron density map was computed with structure factors between 20 and 8 Å resolution. Data were recorded on photographic films by oscillation photography at the Cornell High Energy Synchrotron Source. 574 films were indexed and intensities were estimated for 4 411 246 observations measured 3 σ above the background to 2.7 Å resolution. 2 626 720 reflections were unique accounting for 81% of data to 8 Å resolution and 43% of the data to 2.8 Å. The overall scaling agreement factor was 12.3%. An initial set of phases for data between 20 and 15 Å were calculated from the Fourier transform of a spherical shell of inner and outer radii of 139 and 192 Å respectively placed in the NωV unit cell. These phases were refined by real space molecular averaging procedures. The phases were extended to 8 Å resolution in steps of one reciprocal lattice point, followed by 5–6 cycles of density averaging. The handedness of the map was determined by calculating difference Fourier between native data and data collected on the crystals of NωV soaked in 2–5 mM flourecene mercury acetate. The mercury atoms were identified (Table 2) in the negative electron density suggesting the Babinet opposite (phase = phase + 180) solution for the phases. The electron density map at 8 Å was computed with observed amplitudes and phases for the correct hand and compared with the BBV based $T = 4$ model structure identified in bold. **a** A stereoview of the electron density in the helical interior of NωV with the adjusted BBV model superimposed. The γ peptide Cα positions are shown. Note their proximity to the rod-shaped electron density characteristic of a helix. **b** A stereoview of electron density close to the fivefold symmetry axes displaying a characteristic feature observed in both BBV and NωV electron density. The chemical nature of this "doughnut" feature has not been determined in BBV or NωV. Note the proximity of the loops defined by Cα positions from the adjusted BBV coordinates. The same relation between this density feature and the βD-βE loop (closest to ring shaped density) is seen in the BBV structure

References

1. Goldbach R (1987) Genome similarities between plant and animal RNA viruses. Microbiol Sci 4: 197–202
2. Rossmann MG, Johnson JE (1989) Icosahedral RNA virus structure. Annu Rev Biochem 58: 533–573
3. Rossmann MG, Rueckert RR (1987) What does the molecular structure of viruses tell us about viral functions? Microbiol Sci 4: 206–214
4. Chen Z, Stauffacher C, Li Y, Schmidt T, Bomu W, Kamer G, Shanks M, Lomonossoff G, Johnson JE (1989) Protein-RNA interactions in an icosahedral virus at 3.0 Å resolution. Science 245: 154–190
5. Hosur MV, Schmidt T, Tucker RC, Johnson JE, Gallagher TM, Selling BH, Rueckert RR (1987) Structure of an insect virus at 3.0 Å resolution. Proteins Struct Funct Genet 2: 167–176
6. Prasad BVV (1992) The structure of a calcivirus by cryo-electron microscopy (pers. comm.)
7. Hendry DA (1991) Nodaviridae of invertebrates. In: Kurstak E (ed) Viruses of invertebrates. Marcel Dekker, New York, pp 227–276
8. Moore NF (1991) The *Nudaurelia* β family of insect viruses. In: Kurstak E (ed) Viruses of invertebrates. Marcel Dekker, New York, pp 277–285
9. Newman JFE, Brown F (1977) Further physicochemical characterization of Nodamura virus. Evidence that the divided genome occurs in a single component. J Gen Virol 38: 83–95
10. Friesen P, Rueckert RR (1981) Synthesis of black beetle virus proteins in cultured Drosophila cells: differential expression of RNAs 1 and 2. J Virol 37: 876–886
11. Newman JFE, Brown F (1973) Evidence for a divided genome in Nodamura virus, an arthropod-borne picornavirus. J Gen Virol 21: 371–384
12. Mori K-I, Nakai T, Muroga K, Misao A, Mushiake K, Furusawa I (1992) Properties of a new virus belonging to Nodaviridae found in larval striped jack (*Pseudocaranx dentex*) with nervous necrosis. Virology 187: 368–371
13. Gallagher TM, Rueckert RR (1988) Assembly dependent maturation cleavage in provirions of a small icosahedral insect ribovirus. J Virol 62: 3399–3406
14. Dasmahapatra B, Dasgupta R, Saunders K, Selling B, Gallagher T, Kaesberg P (1986) Infectious RNA derived by transcription from cloned cDNA copies of the genomic RNA of an insect virus. Proc Natl Acad Sci USA 83: 63–66
15. Schneemann A, Dasgupta R, Johnson JE, Rueckert RR (1993) Use of recombinant baculoviruses in synthesis of morphologically distinct viruslike particles of Flock House virus, a nodavirus. J Virol 67: 2756–2763
16. Schneemann A, Zhong W, Gallagher TM, Rueckert RA (1992) Maturation cleavage required for infectivity of a nodavirus. J Virol 66: 6728–6734
17. Fernandez-Tomas CB, Baltimore D (1973) Morphogenesis of poliovirus. J Virol 12: 1122–1130
18. Struthers JK, Hendry DA (1974) Studies of the protein and nucleic acid components of *Nudaurelia capensis* β virus. J Gen Virol 22: 355–362
19. du Plessis DH, Mokhosi G, Hendry DA (1991) Cell free translation and identification of the replicative form of *Nudaurelia* β virus RNA. J Gen Virol 72: 267–273
20. Olson NH, Baker TS, Johnson JE, Hendry DA (1990) The three-dimensional structure of frozen hydrated *Nudaurelia capensis* β virus, a $T = 4$ insect virus. J Struct Biol 105: 111–122

21. Reinganum C (1991) Tetraviridae. In: Adams JR, Bonami JR (eds) Atlas of invertebrate viruses. CRC Press, Boca Raton, pp 387–392
22. Agrawal DK, Johnson JE (1992) Sequence and analysis of the capsid protein of *Nudaurelia capensis* ω virus, an insect virus with $T = 4$ icosahedral symmetry. Virology 190: 806–814
23. Caspar DLD, Klug A (1962) Physical principals in the construction of regular viruses. Cold Spring Harbor Symp Quant Biol 27: 1–24
24. Johnson JE, Fisher AJ (1993) Principles of virus structure. In: Webster RG, Granoff A (eds) Encyclopedia of virology. Academic Press, London, in press
25. Harrison SC, Olson AJ, Schutt CE, Winkler FK, Bricogne G (1978) Tomato bushy stunt virus at 2.9 Å resolution. Nature 276: 368–373
26. Abad-Zapatero C, Abdel-Meguid SS, Johnson JE, Leslie AGW, Rayment I, Rossmann MG, Suck D, Tomitake T (1980) Structure of southern bean mosaic virus at 2.8 Å resolution. Nature 286: 33–39
27. Williams R (1979) The geometrical foundation of natural structure. Dover, New York
28. Fisher AJ, Johnson JE (1992) Ordered duplex RNA controls capsid architecture in an icosahedral animal virus. Nature 361: 176–179
29. von Bonsdorff C, Harrison S (1975) Sindbis virus glycoproteins form a regular icosahedral surface lattice. J Virol 16: 141–145
30. Choi H-K, Tong L, Minor W, Dumas P, Boege U, Rossmann MG, Wengler G (1991) Structure of Sindbis virus core protein reveals a chymotrypsin-like serine proteinase and the organization of the virion. Nature 354: 37–43
31. Finch JT, Crowther RA, Hendry DA, Struthers JK (1974) The structure of *Nudaurelia capensis* β virus: the first example of a capsid with icosahedral surface symmetry $T = 4$. J Gen Virol 24: 191–200
32. Sehnke P, Harrington M, Hosur M, Li Y, Usha R, Tucker R, Bomu W, Stauffacher C, Johnson J (1988) Crystallization of viruses and virus proteins. J Crystal Growth 90: 222–230.35
33. Cavarelli J, Bomu W, Liljas L, Kim S, Minor W, Munshi S, Muchmore S, Schmidt T, Johnson J (1991) Crystallization and preliminary structure analysis of an insect virus with $T = 4$ quasi-symmetry: *Nudaurelia capensis* ω virus. Acta Crystallogr B47: 23–29
34. Fisher A, McKinney B, Schneeman A, Rueckert RR, Johnson JE (1993) Crystallization of virus-like particles assembled from Flock House virus coat protein expressed in a baculovirus system. J Virology 67: 2950–2953
35. Zlotnick A, Reddy V, Schneemann A, Dasgupta R, Rueckert R, Johnson J (1993) A buried aspartic acid catalyzes autoproteolytic maturation in a family of insect viruses (in prep.)
36. Olson N, Baker T (1989) Magnification calibration and the determination of spherical virus diameters using cryo-microscopy. Ultramicroscopy 30: 281–298
37. Crowther R, DeRosier D, Klug A (1970) The reconstruction of a three-dimensional structure from projections and its application to electron microscopy. Porch Roe Soc Loaned A317: 319–340
38. Fuller S (1987) The $T = 4$ envelope of Sindbis virus is organized by interaction with a complimentary $T = 3$ capsid. Cell 48: 923–934
39. Baker T, Drak J, Bina M (1988) Reconstruction of the three dimensional structure of Simian virus 40 and visualization of the chromatin core. Proc Natl Acad Sci USA 422–426

40. Franks A (1955) An optically focusing X-ray diffraction camera. Proc Phys Soc Sect B 68: 1054–1064
41. Harrison S (1968) A point focusing camera for single crystal diffraction. J Appl Crystallogr 1: 84–90
42. Schmidt T, Johnson J, Phillips W (1983) The spherically averaged structures of cowpea mosaic virus components by X-ray solution scattering. Virology 127: 65–73

Authors' address: Dr. J. E. Johnson, Department of Biological Sciences, Purdue University, West Lafayette, IN 47907, U.S.A.